Integrated Modelling of Sawtooth Oscillations in Tokamak Plasmas

F. Porcelli [1], G. Bateman[2], L.-G. Eriksson[3], D. Grasso [1], J. Graves [4], T. Hellsten [5], G. Huysmans [3], T. Johnson[5], A. Kritz [2], H. Lütjens [6], M.-L. Mayoral [7], M.F. Nave [8], C. N. Nguyen [2], A. Pankin [9], A. Perona [1], S. D. Pinches [7], P. Sandquist [10], O. Sauter [4], S. Sharapov [7], I. Voitsekhovich [8], F. Zonca [11], contributors to JET-EFDA [12] and to the European Task Force on Integrated Modelling Activity [13]

[1] Burning Plasma Research Group, Department of Energetics, Politecnico di Torino, Italy
[2] Lehigh University Physics Department, Bethlehem, PA 18015, USA
[3] Association EURATOM-CEA, CEA/DSM/DRFC, CEA-Cadarache, France
[4] CRPP, Association EURATOM-Confederation Suisse, EPFL, 1015 Lausanne, Switzerland
[5] Alfvén Laboratory, Association VR-Euratom, Stockholm, Sweden
[6] CPHT Ecole Polytechnique, UMR-7644 du CNRS, Palaiseau, France
[7] Euratom/UKAEA Fusion Association, Culham Science Centre, Abingdon OX14 3DB, UK
[8] Euratom/IST Fusion Association, Centro de Fusao Nuclear, Lisboa, Portugal
[9] SAIC, San Diego, CA 92121, USA
[10] Euratom/VR Fusion Association, Chalmers Univ. of Technology, Goteborg, Sweden
[11] Association Euratom/ENEA/CNR Fusione, Frascati, Italy
[12] See Appendix of J.Pamela et al, *Proc. 20th IAEA Fus. En. Conf. 2004 (Vilamoura)*
[13] http://www.efda-taskforce-itm.org

e-mail contact of main author: porcelli@polito.it

Abstract. The present understanding of sawtooth oscillations in tokamak plasmas is discussed. Predictive sawtooth modelling requires the integration of various aspects of tokamak physics, including transport, heating and current drive, MHD stability, kinetic effects and fast particle dynamics. In particular, fast particle distributions must be obtained self-consistently, taking into account auxiliary heating, fusion-produced alpha particles and the redistribution of fast ions due to sawtooth crashes and the relevant fast particle driven instabilities. The model proposed here is shown to be in fair quantitative agreement with experimental data and to provide a useful tool for the definition of a possible strategy for sawtooth control in fusion burning plasmas.

1. Introduction

The work discussed in this paper is based on a model for the prediction of the sawtooth period and amplitude, originally proposed in 1996 in [1]. In essence, this model provides a condition for triggering sawtooth crashes, based on the linear stability threshold of internal modes with toroidal n=1 and dominant poloidal m=1 mode numbers, and a prescription for the recalculation of the q and pressure profiles after a sawtooth relaxation, both of relatively easy implementation in transport codes. Initial comparisons of the model predictions with data from TCV, FTU and JET tokamak experiments were fairly encouraging [2,3]. However, the evaluation of the linear stability threshold requires accurate knowledge the plasma geometrical parameters and of several plasma profiles, including thermal plasma and fast particle profiles, which in turn are affected by the sawtooth dynamics itself.

In this paper, several recent advances are discussed: (i) a comparison of the model prediction with data from TFTR and JET experiments; (ii) improved expressions for the linear stability

threshold, most notably, for the ideal MHD and fast particle energy functionals; (iii) sawtooth control by ICCD; (iv) the development of a particle-following numerical tool for assessing the effect of m=1 internal perturbations on fast ion orbits; (v) a possible role of energetic electrons on the appearance of *grassy sawteeth* observed on JET. The concluding section outlines the limitations of the present model and possible directions for further improvements.

2. Testing the sawtooth model against experimental data

The sawtooth model has been implemented in various transport codes, including ASTRA, JETTO, TRANSP, BALDUR, and is now available as a Fortran module in the National Transport Code Collaboration Module Library (http://w3.pppl.gov/NTCC). The model for partial magnetic reconnection, also proposed in [1], has been implemented as an option in the NTCC KDSAW module, which is used to compute changes in the plasma profiles after each sawtooth crash.

Integrated BALDUR simulations of 5 JET H-mode and 12 TFTR L-mode discharges were used to calibrate and test the model [4]. It was found that in these discharges sawtooth crashes are usually triggered by an *m*=1 internal mode in the semicollisional regime, as illustrated in Fig. 1. For this resistive mode to trigger a sawtooth crash, the normalized δW has to be larger than the normalized ion gyro-radius, $\triangle$, (solid line rising above the dashed line in the second panel from the bottom in Fig. 1) and a multiple of the semicollisional m=1 mode growth rate, 3γ, has to be larger than the ion diamagnetic frequency, $\triangleright_{*i}$, (dashed line rising above the solid line in the bottom panel). In simulations of some of the discharges, sawtooth crashes are triggered by the effect of NBI fast ions on the internal *m*=1 mode [4]. In most of the simulations the sawtooth period increases with increasing magnetic reconnection fraction. Figure 2 gives a pictorial example of the partial reconnection model used in the simulations (for a mathematical description, see [1]). Since a model is not yet available to predict the magnetic reconnection fraction within integrated simulations, the magnetic reconnection fraction is used as a parameter to calibrate the sawtooth period in the simulations. The sawtooth period is also found to increase with increasing heating power when the power deposition profile is sufficiently broad. Time intervals with constant heating power are used to determine the sawtooth period. In the discharge considered in Fig. 1, for example, the heating power increases from about 1 MW between 13 and 14.5 seconds to about 3.5 MW between 14.5 and 16 seconds, and it can be seen that the sawtooth period increases at 14.5 seconds.

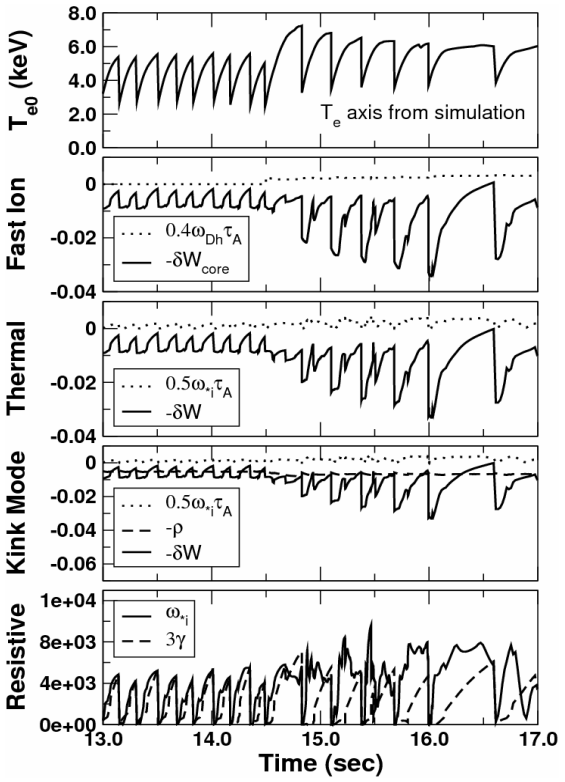

Figure 1: *Triggering conditions for sawtooth crashes in a BALDUR simulation of JET 33131 with 40% magnetic reconnection. The time evolution of the central electron temperature is shown in the top panel while components of the sawtoothi trigger condition are shown in the other four panels.*

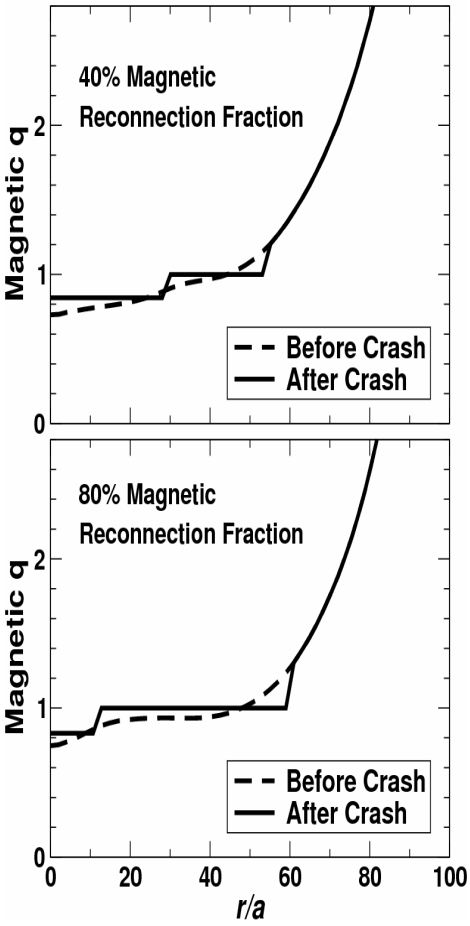

Figure 2: *Magnetic q profile as a function of minor radius just before and just after a sawtooth crash in simulations of JET discharge 33131 with 40% (top panel) and 80% (bottom panel) magnetic reconnection fraction.*

There is significant random variation in the sawtooth periods within each time interval in both the simulations and the experimental data. Consequently, we compared the median sawtooth period in each simulation with the corresponding quantity from experimental data. For the 20 time intervals within the 17 discharges simulated, the best average agreement with experimental data was obtained with approximately 37% magnetic reconnection fraction. This result was obtained using the MMM95 transport module (http://w3.pppl.gov/NTCC) within the BALDUR integrated modeling code. It is anticipated that this result will depend on the transport model and power deposition profile that is used, particularly within the sawtooth mixing region.

3. δW expressions for Sawtooth Modelling Modules

This section details and develops accurate analytic expressions for the potential energy of the internal kink mode. Particular attention is given to ideal MHD and ideal kinetic contributions to stability. Issues dealt with include finite magnetic shear, finite pressure and elongation. The ultimate goal is to provide expressions which involve only radial integrals. This will enable rapid evaluation of the kink mode stability criteria at every time-step of a transport code (e.g. ASTRA and JETTO). Thus, poloidal angle, energy, and pitch angle integrals are calculated analytically.

Let us start with the kinetic contribution from alpha particles. The following δW normalisations will be employed: $\gamma_I \tau_A = (\pi / s_1)\delta W = \delta W^P$, where δW^P is the normalisation used in [1]. For alpha particles in ITER it is sufficient to assume an isotropic distribution function, zero orbit widths and zero flow shear. Taking into account finite shear, finite elongation and pressure in the toroidal magnetic drift one can show that:

$$\delta\hat{W}_\alpha = -\frac{3}{8}\left(\frac{r_1}{R_0}\right)^{3/2}\left(\frac{2\mu_0}{B_\theta^2(r_1)}\right)\int_0^{r_1} dr\left(\frac{r}{r_1}\right)^{3/2}\left(\frac{2}{1+\kappa}\right)^2\frac{dP_\alpha}{dr}\left(\frac{2^{3/2}}{\pi}F_k(r)\right)$$

where κ is the elongation, r_1 is the q=1 radius, P_α is the alpha particle pressure and the real part of F_k is given by :

$$F_k(r) = \Re\left\{\int_0^1 dk^2 \frac{F_q^2}{F_1\left(\frac{2}{1+\kappa}\right) + 2sF_2 - \zeta\left(\frac{1}{4q^2} + F_3\right)}\right\}$$

where F_q and $F_{1,2,3}$ are e.g. defined in [5], and q, s and ζ are respectively the safety factor, the magnetic shear and ballooning parameter. The goal is to obtain F_k as a function of r for a wide

variety of plasma conditions. A fit which has an error of less than 5 percent over $0 < s < 1$ and $0.7 < q < 1$, $0 < \zeta < 0.2$, and $0 < \kappa < 1.4$ is given by:

$$F_k = \left(\frac{2}{1+\kappa}\right)\left(1+\frac{3(1+\kappa)}{8}\zeta\right)\frac{0.67-4.75x+17.63x^2-10.06x^3+2.18x^4}{1-4.61x+15.51x}\times$$
$$\left[1+(1-q)\{1+40(1-q)^4(1-\exp(10x))\}\left\{\frac{5.88-20.54x+32.71x^2}{1-5.87x+17.97x^2}\right\}\right],$$

where $x = (1+\kappa)(s - 3\xi/4)/2$. Here, F_k varies by more than a factor of two over typical plasma parameters. Hence, in terms of the notation of [1] (see Eqs. (B.8) and (27)):

$$\delta W_\alpha^P = -\frac{1}{s_1}\epsilon_1^{3/2}\beta_{p\alpha}^* \qquad \text{with} \qquad \beta_{p\alpha}^* = \left(\frac{2\mu_0}{B_\theta^2(r_1)}\right)\int_0^{r_1} dr\left(\frac{r}{r_1}\right)^{3/2}\frac{dP_\alpha}{dr}\left(\frac{2^{3/2}\cdot 3}{8}F_k(r)\right)$$

which thus serves to correct the expression in [1] where $2^{3/2}\ 3\ F_k / 8=1$ is used.

Let us now consider the MHD contributions to the internal kink mode, focussing on the effects of toroidicity and shaping on the ideal internal kink mode. The well known Bussac analytical relation [6] for toroidal internal kink stability is valid only for finite magnetic shear and large aspect ratio. Similar limitations apply to [7,8], which treat plasma shaping effects. Two approaches can be followed in order to improve on earlier works. One approach [9] exploits parameter fitting of linear MHD codes, with ideally, self consistent coupling to equilibrium codes. The advantage of this method enables investigation of extreme shapes and spherical plasmas. An example is shown in Fig. 3(a) where the fitted equation

$$\gamma^{\text{fitl}}\tau_A = 0.45\frac{\epsilon_1\kappa_1}{1+7\epsilon_1 s_1}(\beta_{p1}-\beta_{p1}^{c,\text{fitl}}), \qquad (1)$$
$$\beta_{p1}^{c,\text{fitl}} = 0.7-0.5\kappa_1.$$

is compared with the results obtained from the KINX code over a very wide range of shaping parameters and inverse aspect ratio. Another approach [10] extends analytical theory to accommodate realistic plasmas. This method retains subtle parameterisation which can be lost when doing only numerical scans. An example of this for a particular two-parameter safety factor

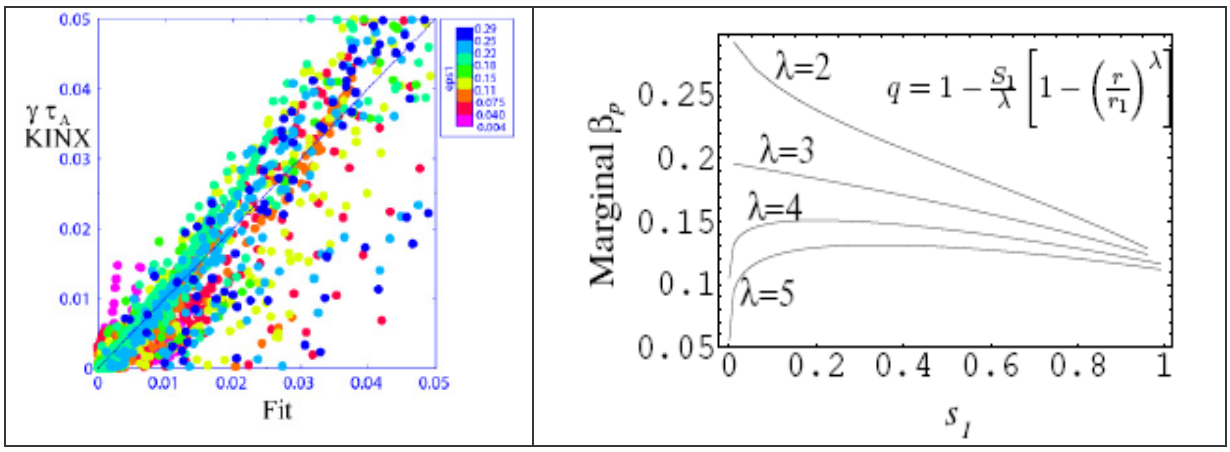

(a) (b)

Figure 3*: Showing (a) the comparison of Eq. (1) with the growth rate from KINX over a wide range of plasma parameters [9], and (b) the marginal poloidal beta in a toroidal plasma as a function of shear at q=1 for differing λ. The latter is calculated from analytical corrections to the well known formula of Ref. [6].*

is shown in Fig. 3(b). The new analytical formula from which the curves in Fig. 3(b) are generated serves to correct that given in [6], for which the marginal poloidal beta is approximately 0.3. Work continues on improving the analytical calculations through taking into account additional neighbouring sideband harmonics [10].

4. Sawtooth control by ICCD

An important question is to what extent it is possible to destabilise fast ion induced long sawteeth. Most experiments aimed at affecting the sawtooth period by modifying the shear near the $q = 1$ surface have been carried out in plasmas with little or no fast ion pressure inside the $q = 1$ surface. In order to study the effect of a shear modification using Ion Cyclotron Current Drive (ICCD) on fast ion induced long sawteeth, a number of experiments were carried out at JET during 2003. In these experiments a central fast ion pressure was first created by applying hydrogen minority ICRF heating with a near on-axis resonance. Moreover, a phasing of the antennas that produces predominantly co-current propagating waves was used to increase the peaking of the fast ion pressure profile via the ICRF induced "pinch effect" [11]. The ICCD was then applied, which had a hydrogen cyclotron resonance on the high field side of the magnetic axis near the $q = 1$ surface and an antenna phasing launching waves propagating primarily in the counter current direction. Thus, the available ICRF power at JET was split on the two tasks of creating a fast ion pressure in the centre and destabilising the resulting fast ion induced long sawteeth with ICCD. The experiments showed that it was indeed possible to shorten the sawteeth by the application of ICCD, and they also indicated that process is rather sensitive to the exact distance between the $q = 1$ surface and the ICCD cyclotron resonance layer [12]. The effect of the ICCD on the driven currents and the fast ion pressure profiles has recently been analysed and is reported in [13]. The analysis is based on simulations with the SELFO codes, which combines a full wave solver for the wave electric field and a 3D Fokker-Planck Monte Carlo solver for the distribution function of the resonating ions. The latter includes finite orbit width effects, and the SELFO code produces a self-consistent solution to the two problems. The analysis with the SELFO code shows quite clearly that the shear near the $q = 1$ surface was significantly increased in the discharge where the application of ICCD produced a significant shortening of the sawteeth in the presence of a central fast ion pressure. Moreover, it was shown that the ICCD had a very small effect on the fast ion pressure inside the $q = 1$ surface, whereas it increased it outside. A more thorough analysis, based on the SELFO simulations, of the influence of shear profile and the change in the fast ion pressure profiles during application of ICCD on the sawtooth stability has started [14].

5. Particle-following numerical tools for assessing the effects of MHD perturbations on fast ion orbit distributions

The effects of low-frequency MHD-modes on fast ions, such as fast ion mixing during a sawtooth crash, are of major concern for the burning plasma devices. In order to assess such effects in a unified way, the drift orbit particle-following HAGIS code [15] used for the studies of high-frequency Alfvénic modes on resonant ions has been extended in order to display Poincaré plots for both the magnetic field lines and drift orbits of fast ions in the presence of finite amplitude MHD perturbations. This allows assessing both the regular and stochastic behaviour of the fast ions, so that the identification of the stochasticity thresholds for both the magnetic field lines and the drift orbits becomes also possible.

As a series of test cases, the behaviour of fast ions, both trapped and passing, has been investigated for a time 3 10^{-4} s (comparable to sawtooth crash time) in the presence of n=1 kink mode of finite amplitude, either stationary with $\delta B_\theta / B_0 = 5\ 10^{-3}$ or growing linearly from $\delta B_\theta / B_0 = 1\ 10^{-5}$ to $\delta B_\theta / B_0 = 5\ 10^{-3}$. A typical example of JET equilibrium (discharge #60195 at t=11.0 s) was reconstructed with the EFIT and HELENA codes, and the linear unstable n=1 mode was computed with the CASTOR code. The linear eigenfunction was kept fixed at the growing mode amplitude, in order to consider fast ions at the pre-crash time and avoid at this first step the complications associated with a description of the sawtooth reconnection.

In order to prevent irregularities caused by the numerical accuracy, the HAGIS performance has been tested first for some drift orbits of fast ions most sensitive to the accuracy. Figure 4 shows two orbits, which are close to the stagnation orbit, for a fast ion with energy 500 keV in both the unperturbed JET equilibrium (Fig.4(a)) and in the presence of a static kink mode with an amplitude $\delta B_\theta / B_0 = 5\ 10^{-3}$ (Fig.4(b)). The ion orbit does not change its radial position and it stays deeply inside the q=1 surface for the time of the run, but its orbit becomes elongated vertically due to the presence of the kink perturbation.

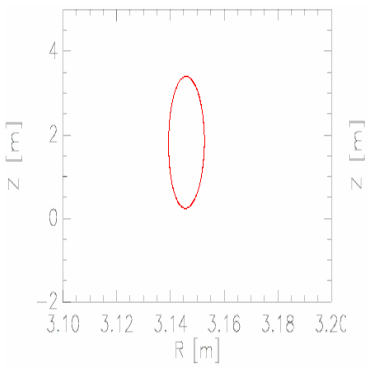

Figure 4(a)

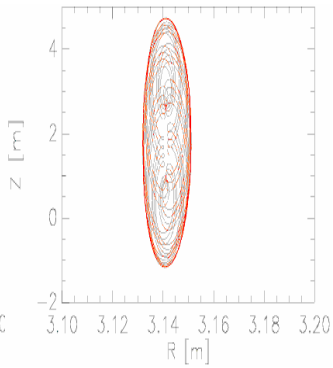

Figure 4(b)

In order to assess the structure of the magnetic field lines, the Hamiltonian description developed, e.g., in [16] has been incorporated in the HAGIS code. Poincaré plots at any toroidal cross-section of a tokamak were then developed for both the magnetic field lines and drift orbits of fast ions. Different types of drift orbits were identified in the presence of a static high-amplitude n=1 kink mode. In particular, it was found that, e.g. a deeply passing 500 keV fast ions may become trapped in the vicinity of the second magnetic axis caused by the n=1 perturbation as Fig. 5(a) shows, or these ions may stay attached to the original magnetic axis as Fig. 5(b) shows (the red dots represent the ion orbit, the blue dots are the perturbed magnetic surfaces, the green line is the q=1 unperturbed surface). However, the probability of trapping of the fast ion by the second magnetic axis, is actually not very high if a mode of linearly growing amplitude is considered. For example, a kink mode growing from $\delta B_\theta / B_0 = 1\ 10^{-5}$ to $\delta B_\theta / B_0 = 5\ 10^{-3}$ can only trapped the ion if it crosses the region of the magnetic "island" at a critical amplitude $\delta B_\theta / B_0 = 2.5\ 10^{-3}$ Effect of n=1 on trapped ICRF fast ions with energy 500 keV was tested then. The pitch angle of such ions was chosen in order for the banana tips to stay on a vertical line passing through

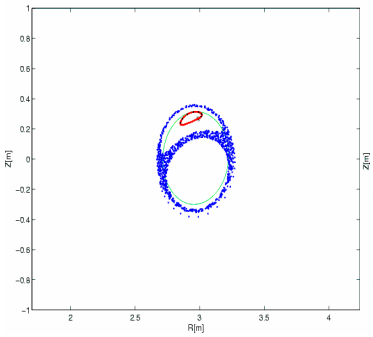

Figure 5(a)

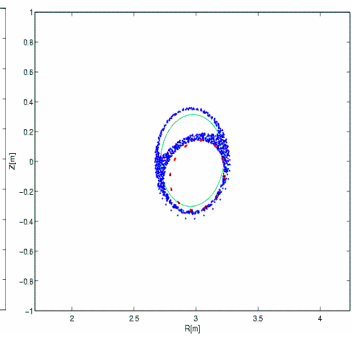

Figure 5(b)

the magnetic axis corresponding to the on-axis ICRF heating. It was found that the trapping effect due to the second magnetic axis is not important for the ICRF-heated ions and these ions in general are not affected by the n=1 kink perturbation.

The problem of the evolution of fast ion orbits during internal kink perturbations was also addressed in [17]. However, the orbits obtained with the HAGIS code seems to be more complex. Furthermore, Ref. [17] did not address the possible effects of magnetic stochasticity.

6. Supra-thermal electrons and grassy sawteeth on JET

The acceleration of electrons and ions by electric fields triggered during magnetic reconnection is one of the most important problems in plasma physics, as recognised long time ago [18]. For magnetic reconnection caused by sawtooth crashes, the possibility of electron acceleration by the pulsed parallel electric field has been first assessed theoretically in [19]. More recently, intense X-ray bursts have been discovered experimentally on the T-10 tokamak with a system of X-ray detectors viewing the plasma tangentially [20]. These X-ray bursts were associated with a population of supra-thermal electrons of energy $E \approx 30 \div 100$ keV accelerated by electric fields arising during the magnetic reconnection around the X-points of the magnetic islands.

An interesting new type of sawteeth, so-called "grassy sawteeth", is observed in JET plasmas with high-power ICRF-heating instead of the usual "monster" sawtooth, if the plasma density falls below a critical value of about $n_e(0) < 2\ 10^{19}$ m^{-3} [21, 22]. The grassy sawtooth regime is characterised by the sawtooth period, which is few times shorter than the monster sawtooth period, while the reconnection time is about order of magnitude longer in the grassy sawtooth. An explanation of the grassy sawteeth is searched for on the basis of the following observations, indicating that a supra-thermal electron population surrounding the q=1 magnetic surface may determine this highly unusual sawtooth behaviour: (i) enhanced fast electron Bremsstrahlung is observed during the grassy sawteeth phase [23], and (ii) because of the relatively low plasma density, the inductive steady-state parallel electric field in the central region of the JET plasma becomes close to the critical electric field, at which electrons travelling near the speed of light can run away. Under these conditions, the pulsed sawtooth reconnection electric field, which for grassy sawteeth becomes comparable to Dreicer electric field, can generate a suprathermal electron population in the vicinity of the q=1 magnetic surface repeatedly at each sawtooth crash. Under the condition (ii), however, the near-threshold electric field prevents a rapid deceleration of the suprathermal electrons due to Coulomb collisions, so that a suprathermal electron current may be present for a time long enough to affect the stability of the next sawtooth.

In order to assess the fast electron behaviour in a plasma with a near-critical parallel electric field satisfying condition (ii), a Fokker-Planck equation has been derived and solved in local analysis for the steady-state relativistic electron distribution function [24]. The relevant expressions describing the electron velocity distribution function up to the relativistic region were obtained for parallel electric field either below or above the critical value. The combined steady-state near-critical electric field and the pulsed electric fields appearing repeatedly during every sawtooth crash will be a next subject in explaining the grassy sawteeth, with the study of a possibility for grassy sawteeth to occur in burning plasma of ITER.

7. Conclusions

In conclusion, we have presented a model for the prediction of the sawtooth period and amplitude. This model, originally proposed in [1], has been further developed and tested against experimental data. The model is capable of reproducing the experimental sawtooth period within a factor of two. More importantly, the model is able to capture trends, such as the lengthening of the sawtooth period during NBI injection, and can be used in order to assess possible strategies for sawtooth control. In this respect, it is encouraging that techniques such as ICCD localized near the q=1 surface are shown to be effective in inducing sawtooth crashes and therefore produce relatively mild sawteeth.

In spite of the success, it is important to point out limitations and directions for further improvements. The sawtooth model is based on the linear stability threshold for m=1 modes, including realistic effects and actual geometric factors. However, it is clear from experiments that sometimes relatively large amplitude m=1 oscillations are present on the sawtooth ramp long before the crash occurs. In this case, the use of a linear stability threshold is questionable.

The open scientific question is what determines the occurrence of partial reconnection, i.e., why the plasma temperature is relaxed throughout the central region in spite of the fact that q on axis remains below unity. The partial reconnection model proposed in [1] is partly heuristic and does not provide a satisfactory answer to this question. It appears that often-times a secondary instability is excited during the growth of the m=1 magnetic island, possibly related to the steep pressure gradients that tend to form across the island separatrix. Thus, the instability may be of the ballooning or interchange type. Further thoughts and numerical investigations are needed to clarify this point. Eventually, the goal is to come up with a partial reconnection model that does not present any free parameters, such as the fraction of reconnected flux.

References

[1] F. Porcelli, D. Boucher, M.N. Rosenbluth, Plasma Phys. Control. Fusion **38** (1996) 2163 .
[2] O. Sauter et al, Phys. Rev. Lett. **88** (2002) 105001-1 ; C. Angioni et al, Nuclear Fusion **43 (**2003) 455.
[3] S. Cirant *et al* Plasma Phys. Control. Fusion **41** (1999) B351.
[4] G. Bateman, C.N. Nguyen, A.H. Kritz, F.Porcelli, Phys. Plasmas **13** (2006) 072505.
[5] J. Graves and R. J. Hastie, Plasma Phys. Control. Fusion **42** (2000) 1049.
[6] M. N. Bussac *et al,* Phys. Rev. Lett. **35** (1975) 1638.
[7] D. Edery and G. Laval, Phys. Fluids **19** (1976) 260.
[8] H. G. Eriksson and C. Wahlberg, Phys. Plasmas **9** (2002)] 1606.
[9] A. Martynov, J. Graves, O. Sauter, Plasma Phys. Control. Fusion **47** (2005) 1743.
[10] J. Graves and C. Wahlberg, to be published.
[11] L.-G. Eriksson et al., Phys. Rev.Lett. **81**, 1231 (1998) ; M. Mantsinen et al., Phys. Rev. Lett. **91**, 115004 (2002).
[12] L.-G. Eriksson et al., Phys. Rev. Lett. **92**, 235004 (2004).
[13] L.-G. Eriksson et al., Nuclear Fusion **46**, S951 (2006).
[14] J. Hedin et al., Nuclear Fusion **42**, 527 (2002).
[15] S. D. Pinches *et al*, PhD Thesis, University of Nottimgham, UK (1996).
[16] R. Balescu, M. Vlad and F. Spineanu, Phys. Rev. E **58** (1998) 951.
[17] Ya. I. Kolesnichenko et al., Nuclear Fusion **40**, No. 7 (2000).
[18] S. I. Syrovatskii, Sov. Astronom. Journal **43** (1966) 340.
[19] A. V. Gurevich et al., Proc. 11th EPS Conf., Aachen, 1983, v. **7D**, Part II, p.267.
[20] P. V. Savrukhin et al, Proc. 28th EPS Conf., Funchal, 2001, Vol. **25A**, p.1421.
[21] M. Mantsinen *et al*., Plasma Phys. Contr. Fusion **42** (2000) 1291.
[221] S. Sharapov *et al*., Nuclear Fusion **45** (2005) 1168
[23] P. Sandquist *et al*., Proc. 28th EPS Conf., Tarragona, 2005, Vol. **29C**, Paper ID D-1.006.
[24] P. Sandquist *et al*., Phys Plasmas **13** (2006) 072108.